17th World Conference on Earthquake Engineering, 17WCEE
Sendai, Japan - September 13th to 18th 2020

REDUCING RESIDUAL DRIFT WITH MULTISTAGE BUCKLING-RESTRAINED BRACES

B. Sitler[(1)], T. Takeuchi[(2)]

[(1)] *PhD candidate, Tokyo Institute of Technology, sitler.b.aa@m.titech.ac.jp*
[(2)] *Professor, Tokyo Institute of Technology, takeuchi.t.ab.m.titech.ac.jp*

Abstract

Buckling-restrained braces (BRB) are energy dissipating members widely used to achieve a code minimum seismic design. Nevertheless, well-designed BRBs poses excellent ductility, exhibit a stable hysteresis at large drifts, and are capable of withstanding multiple design level events without fracture. However, the decision to repair or replace a structure following a severe earthquake is often instead governed by nonstructural damage and residual drifts. This is a challenge for simply supported BRB frames (BRBFs), as the post-yield stiffness tends to be low, increasing the susceptibility to drift concentration and providing limited elastic restoring force. Post-tensioned self-centering BRBs and damage tolerant moment frame-BRBFs help mitigate these deficiencies, but impose additional costs due to the longer internal load path and increased number of moment connections, respectively. This paper offers a practical and economic alternative, where a conventional BRB is modified so that the core yields in multiple stages.

The proposed multistage buckling-restrained brace (MS-BRB) consists of parallel decoupled cores with different yield drifts. The low yield point (LYP) core features a material with a smaller yield strain and a shorter yield length, while the high yield point (HYP) core features a material with a larger yield strain and a longer yield length. In this system, residual drifts are controlled by maximizing the HYP core yield drift, which provides the elastic restoring force, while minimizing the LYP core yield drifts, which provides plastic energy dissipation. The yield length differential is essential, as it enables a significant multistage effect to be achieved using ductile mild steel, avoiding the severe isotropic hardening of extremely low yield point steels and relatively poor overstrength and ductility of some high strength steels. However, there are multiple material combinations and core strength proportions that may be feasible, and performance may differ depending on the strong ground motion characteristics and intensity.

This paper presents a numerical study that investigates the performance of low and midrise archetype frames employing MS-BRBs. Core compositions with different materials and yield lengths are modelled to investigate the effect of the LYP/HYP yield drift and force differential. The response under increasing seismic intensities is studied, demonstrating that increasing the HYP core yield drift is most effective in reducing residual drifts, while the LYP core size has a local optima. Acceptable residual interstory drifts are achievable over a much wider range of peak transient drifts and ground motion intensities than in simply supported conventional BRBs. Conversely, the theoretical benefits of extremely low yield point steels such as LY100 are shown to be less effective in foreshock-mainshock sequences due to isotropic hardening, suggesting that A36 or LY225 is more suitable as the LYP core material. Finally, a simple design procedure is proposed, where the required strength for a conventional BRB is matched to the sum of the LYP and HYP gross yield strengths. The proposed MS-BRB offers engineers a compact and efficient device to improve residual drifts, trading some of the excess fatigue capacity to achieve a better post-earthquake repair / replace outcome.

Keywords: Multistage buckling-restrained brace; archetype frame; residual drift

1. Introduction

The repairability of a structure after a major earthquake depends not only on the structural and non-structural damage, but also on the presence of permanent interstory residual drifts, which can lead to a loss of building function if exceeding about 0.5% ~ 1.1% [1, 2]. Therefore, the peak interstory residual drift (referred to as "residual drift") is a key response parameter for simply supported buckling-restrained braced frames (BRBF), which exhibit low post yield stiffness, but excellent ductility and fatigue capacity. One solution in low rise BRBFs is to increase the yield strength, but this is inefficient, as it increases the overstrength forces for capacity-based design and makes poor use of the available fatigue capacity. This paper investigates an alternative solution utilizing a new multistage BRB (MS-BRB) [3], which features low yield point (LYP) cores that dissipate energy at small amplitudes and a parallel high yield point (HYP) core that provides an elastic restoring force. This promotes a centered hysteresis and limits residual drifts by following the established principals of a damage tolerant structure [4], all without increasing the BRB sizes or requiring a moment frame.

The methodology adopted in this paper is to conduct numerical analyses of low and midrise archetype frames with MS-BRBs featuring different core materials and yield lengths, and to compare the seismic response under increasing seismic intensities and different types of ground motions. First, the device composition, characteristic trilinear backbone and experimental performance is reviewed, the archetype frames are designed, and the numerical modelling assumptions reported. Two studies are then conducted using trilinear and nonlinear material models. A parametric study of the idealized trilinear models is used to determine the optimal design of the first yield strength of the LYP core and yield deformation of the HYP core. Next, calibrated nonlinear material models are analyzed under multievent earthquake sequences in order to investigate the effect of isotropic hardening of the low yield point steels used for the LYP core,. Finally, a set of design recommendations is discussed.

1.1 Multistage buckling-restrained brace concept

The proposed MS-BRB device (Fig. 1) is similar to a conventional cruciform BRB, but the core plates are only welded together at the ends. The two outer LYP core plates adopt a shorter yield length (e.g., $L_{y,L} / L_{wp} = 0.5$) and material with lower yield strain (e.g., LY225), yielding at small displacements. Conversely, the yield length of the parallel HYP core plate is set to as long as possible (e.g., $L_{y,H} / L_{wp} = 0.85$), and a ductile high-strength bridge steel (e.g., SA400B) is employed to maximize the yield displacement.

This composition has a significant performance advantage over previous "multi-material" [5] or "hybrid" [6] BRB proposals in that extreme steel grades (e.g., LY100 and SA700), which have undesirable inelastic characteristics, are not required to achieve a significant multistage effect. Similarly, this offers practical advantages over "double yield" [7, 8] and "self-centering" BRBs [9] in that a simple load path is retained and the full core strength is utilized at large drifts, features that make conventional BRBs a competitive system.

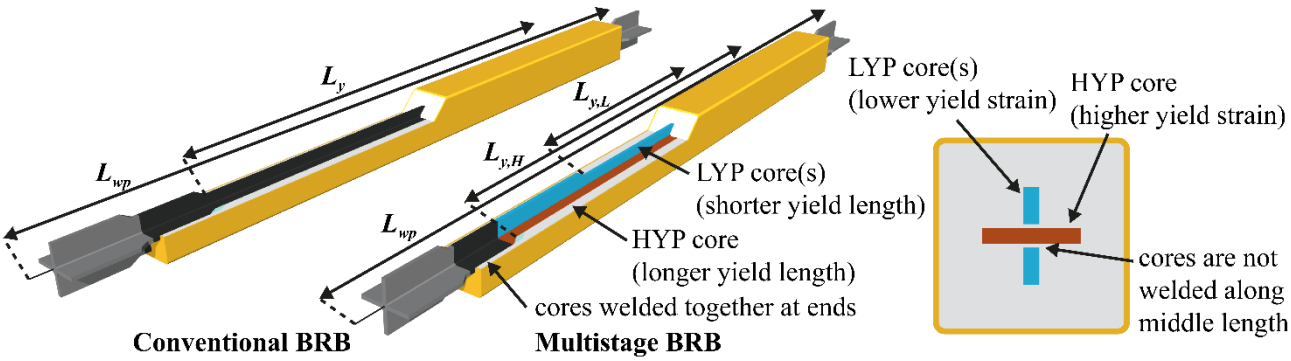

Fig. 1 – Multistage buckling-restrained brace concept

1.2 Experimental validation

The authors have previously tested [3] a specimen with a 384kN gross yield strength at up to 1.5% LYP core average axial strains. Full details of this experiment are outside the scope of this paper, but the core stress-strain response and brace force-displacement hysteresis at key stages are shown below in Fig. 2. The shorter LYP cores experience greater strain demands and yield earlier, while yielding of the HYP core is delayed. This provides 10 ~ 20% supplementary equivalent viscous damping during the 0.4% strain cycles. At large amplitudes after both cores have fully yielded, the hysteresis begins to resemble a conventional high strength BRB. However, the kinematic hardening characteristics of the HYP core material still provide significantly greater post-yield stiffness than steel grades used in conventional BRBs, such as A36 and SN400B.

While an analytical derivation of the trilinear backbone is also outside the scope of this paper, the yield displacements of the LYP ($\delta_{y,L}$) and HYP ($\delta_{y,H}$) cores are distinctly visible. Note that the first yield force ($N_{y,L}$) includes a contribution from both cores and the gross yield strength (N_y) is the sum of the component core yield strengths. These are all design parameters that may be varied by selecting different core materials, yield lengths and areas. The design question is then what combination of $\delta_{y,L}$, $\delta_{y,H}$, $N_{y,L}$ and N_y will result in optimal performance? Also, how does the response of an MS-BRB compare to an equivalent conventional BRB with yield displacement ($\delta_{y,L} < \delta_y < \delta_{y,H}$), and equal initial stiffness (K) and gross yield strength (N_y)?

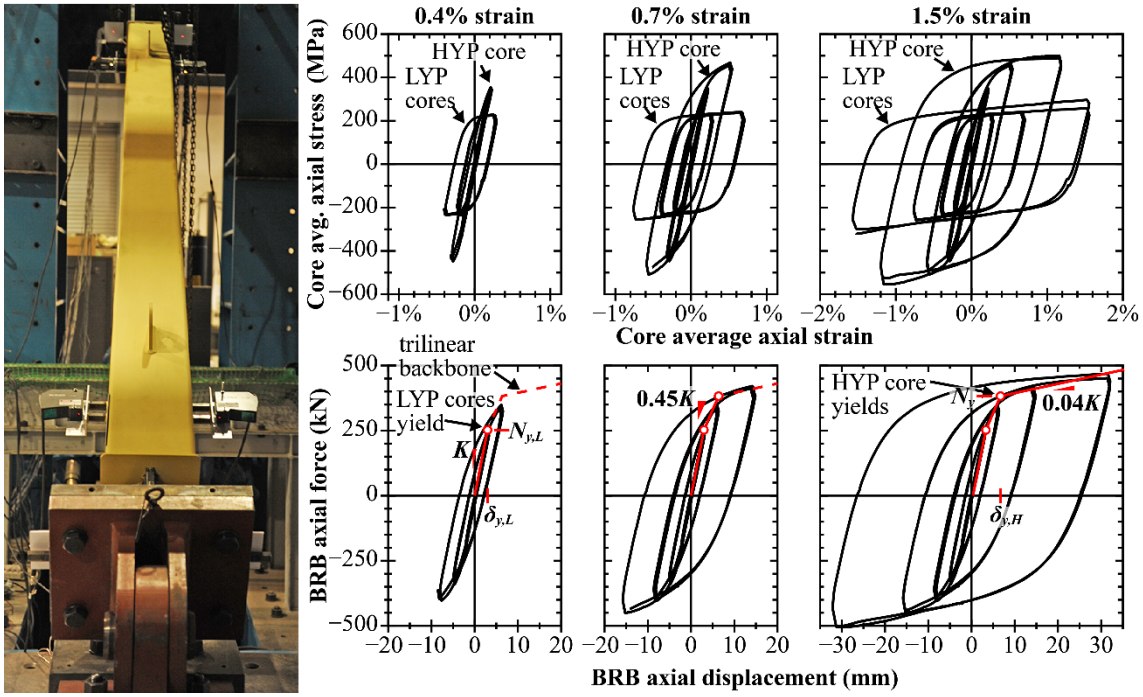

Fig. 2 – Experimental response [3]

2. Numerical model

2.1 Archetype frame

Low rise (3 story) and midrise (6 story) archetype structures were adapted from a previous study [10]. Perimeter elevations were modelled in OpenSees [11] and are shown in Fig. 3. The non-tributary seismic mass was assigned to elastic leaning columns that represent the interior gravity columns, capturing PDelta and continuous column effects. All framing was simply supported, except for the column bases at the BRB gussets, which were fixed and defined as nonlinear fibre members (SN490B, f_y = 385MPa). Mass and tangent stiffness proportional 2% Rayleigh damping was applied to first and second modes. Each BRB was modelled using an assembly of a nonlinear truss element with core area A_y and yield length L_y, and elastic beam-columns with connection area A_e, while the MS-BRBs incorporated additional parallel cores.

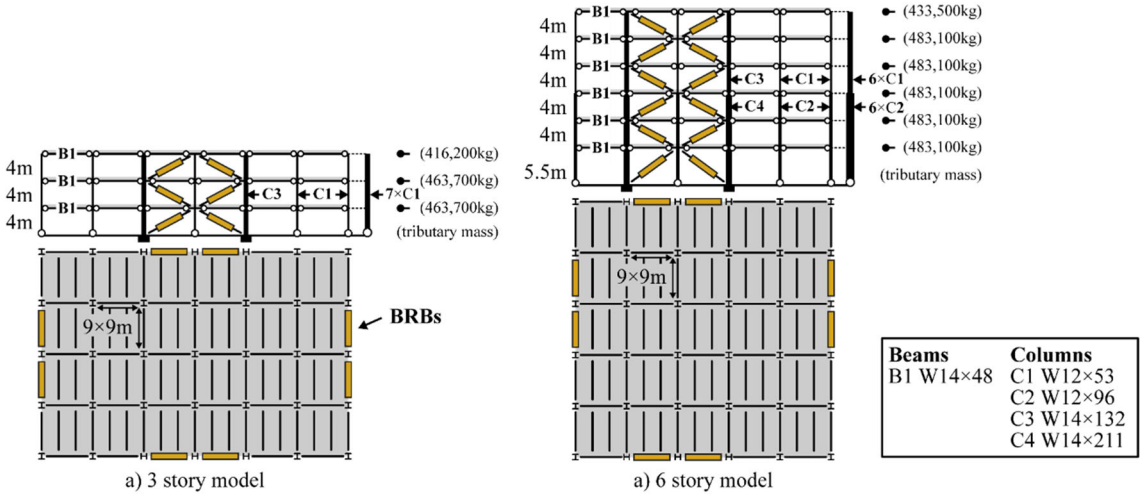

Fig. 3 – Archetype frames

2.2 BRB design

The equivalent lateral force procedure of ASCE 7-16 [12] was followed using design base shear coefficients of 0.23/0.9 (story) and 0.18/0.9 (6 story), based on building periods of T_{3stry} = 0.64s and T_{6stry} = 1.0s. Although the MS-BRB LYP cores yield earlier, the full gross yield strength (N_y) was used to satisfy the required brace force and the initial stiffness held constant for the MS-BRB and BRB designs. This assumes that the inelastic displacement of a MS-BRB will be less than or equal to that of a conventional BRB with equal initial stiffness and gross yield strength, which is validated in this study.

Trilinear (**TRI**) models were designed with first yield strengths set as $N_{y,L}$ / N_y = 0.3 ~ 1.0 (where $\delta_{y,L}$ / δ_y = $N_{y,L}$ / N_y), and the HYP yield displacements set as $\delta_{y,H}$ / δ_y = 1.0 ~ 3.0 (N_y held constant). Nonlinear material models were then designed, including conventional SN400B BRBs (**BRBF**), conventional BRBs with 25% lower strength (**BRBF-L**), and multistage BRBs with LY100+SA440B (**MS-BRBF-L**), LY225+SA440B (**MS-BRBF**) or LY225+SA630B (**MS-BRBF-H**). The core materials and proportions are listed in Table 1, with δ_y referring to **BRBF** models' yield displacement, and the core areas (A_y or $A_{y,L}$+$A_{y,H}$) in Table 2.

Table 1 BRB and MS-BRB designs

Model	LYP core(s)		HYP core		$A_{y,H}/A_{y,L}$	A_e / A_y	$N_{y,L}$ / N_y	$\delta_{y,H}/\delta_y$	T (s)	
	Grade	$L_{y,L}/L_{wp}$	Grade	$L_{y,H}/L_{wp}$					3 story	6 story
BRBF-L	SN400B	0.85	-	-	-	3.0	-	-	0.74	1.17
BRBF / TRI	SN400B	0.70	-	-	-	3.0	-	-	0.64	1.01
MS-BRBF-L	LY100	0.60	SA440B	0.85	0.80	2.5	0.32	2.0	0.62	1.00
MS-BRBF	LY225	0.47	SA440B	0.85	0.50	2.5	0.64	2.0	0.64	1.01
MS-BRBF-H	LY225	0.47	SA630B	0.85	0.25	2.5	0.66	2.8	0.63	1.00

Table 2 BRB (A_y) and MS-BRB ($A_{y,L}$+$A_{y,H}$) core areas

		6 story models: core areas (cm^2)					3 story: core areas (cm^2)		
Story	ϕN_y (kN)	**TRI**	**BRBF**	**MS-BRBF-L**	**MS-BRBF**	**MS-BRBF-H**	Story	ϕN_y (kN)	**TRI**
6	1107	38	38	23 + 18	24 + 12	28 + 7	3	1119	38
5	1720	58	58	35 + 28	37 + 18	43 + 11	2	1519	52
4	2272	77	77	46 + 37	48 + 24	57 + 14	1	1803	61
3	2671	91	91	54 + 43	57 + 28	67 + 17			
2	2928	99	99	60 + 48	62 + 31	74 + 18			
1	3275	110	110	67 + 53	70 + 35	82 + 21			

2.3 Constitutive material models

Giuffré-Menegotto-Pinto nonlinear material models were calibrated to coupon test data from [13], with only slight adjustments made to the parameters in [13] in order to match the mean specified yield strengths.

Two low carbon steels were considered (LY100 and LY225). Both feature low specified yield strengths (LY100: $80 \le f_y \le 120$MPa, LY225: $205 \le f_y \le 245$MPa), significant overstrength (LY100: $f_y / f_u \le 0.6$, LY225: $f_y / f_u \le 0.8$) and large monotonic ultimate strains ($\varepsilon_u{}^m \approx 30\%$), while LY100 exhibits severe isotropic hardening. Isotropic hardening of LY100 was better modelled using Steel4, which expands the yield surface with the cumulative plastic strain, while Steel02 was adopted for all the other materials.

Two ductile high strength bridge steels were considered (SA440B, SA630B). These lack a defined yield plateau and exhibit almost pure kinematic hardening. While both of these ductile "B" grades have similar elongations at fracture (SA440B: $\varepsilon_f \ge 26\%$, SA630B: $\varepsilon_f \ge 24\%$) and material overstrength (SA440B: $f_y / f_u \le 0.8$, SA630B: $f_y / f_u \le 0.85$) as SN400B, the ultimate strains tends to be slightly lower ($\varepsilon_u \approx 12\%$), resulting in significantly greater tangent stiffness at small and moderate strains (e.g., $\varepsilon < 3\%$).

For simplicity, compressive overstrength (β) due to Poisson expansion / contraction and higher mode plastic buckling / friction effects was not considered. This is justified as β is low (less than 1.15) in well-designed single story BRBs, and the diagonally configured BRBs are provided in matching pairs. The calibrated constitutive material parameters are detailed in Table 3, and example hysteresis shown in Fig. 4.

Table 3 Constitutive material model parameters

Steel	Model	f_0 (MPa)	E (GPa)	b	R_0	R_1	R_2	a_1	a_2
LY100	Steel4	100	205	0.1%	20	0.89	0.1	*	*
LY225	Steel02	225	205	0.2%	40	0.95	0.1	0.20	9.8
SN400B	Steel02	295	205	0.5%	40	0.95	0.1	0.29	9.8
SA440B	Steel02	540	190	2.0%	41	0.94	0.1	-	-
SA630B	Steel02	750	190	2.5%	42	0.93	0.1	-	-

* LY100 Steel4 isotropic hardening parameters: $b_{iso} = 0.25$, $b_{iso,u} = 0.2\%$, $\rho_{iso} = 2.0$, $R_{iso} = 0.4$

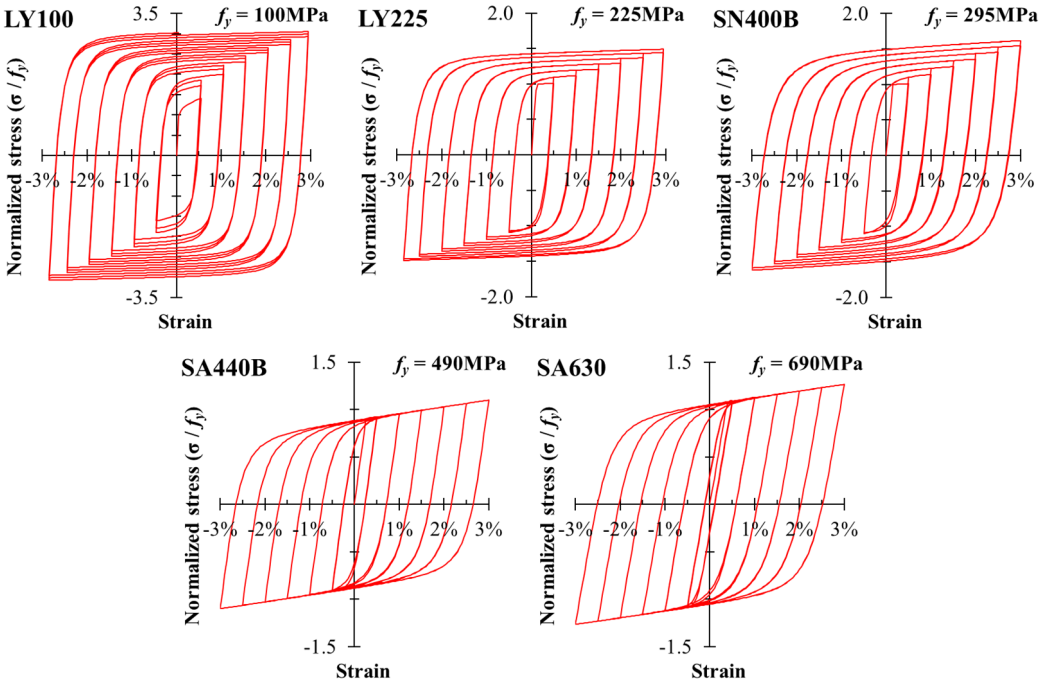

Fig. 4 – Hysteresis of constitutive material models

2.4 Ground motions

Two different ground motions sets were adopted for this study. First, the FEMA 695 far field suite [14] (denoted FEMA 695-FF) was used to study the seismic response under increasing ground motion intensity. Second, multievent earthquake sequences were analysed to determine the influence of isotropic hardening in low yield steels. These include a mainshock-aftershock (Northridge 1994), foreshock-mainshock (Christchurch 2010/2011) and foreshock-foreshock-mainshock-aftershock sequence (Kumamoto 2016). The stronger component of four stations with an approximately design level mainshock were selected.

All records were obtained from the PEER NGA WEST2 (*ngawest2.berkeley.edu*) and NIED K-Net/KiK-Net (*kyoshin.bosai.go.jp*) databases. The event/station/direction details, PEER record sequence numbers (*RSN*) and 5% damped 1-sec spectral accelerations ($S_{a,1s}$) are shown in Table 4, and station/fault locations in Fig. 5.

Table 4 Ground motion sets

FEMA 695 FF

ID	Event/Station/Dir	RSN
FF01	Northr MUL 009	#953
FF02	Northr LOS 000	#960
FF03	Duzce BOL 000	#1602
FF04	Hector HEC 000	#1787
FF05	ImpVall DLT 262	#169
FF06	ImpVall E11 140	#174
FF07	Kobe NIS 000	#1111
FF08	Kobe SHI 000	#1116
FF09	Kocaeli DZC 180	#1158
FF10	Kocaeli ARE 000	#1148
FF11	Landers YER 270	#900
FF12	Landers CLW LN	#848
FF13	LomaP CAP 000	#752
FF14	LomaP G03 000	#767
FF15	Manjil ABBAR L	#1633
FF16	Super ICC 000	#721
FF17	Super POE 270	#725
FF19	ChiChi CHY101 E	#1244
FF20	ChiChi TCU045 E	#1485
FF21	San Fern PEL 090	#68
FF22	Fruili TMZ 000	#125

Northridge 1994 mainshock-aftershock

	17 Jan		**17 Jan~20 Mar**	
Station/Dir	RSN	$S_{a,1s}$	RSN	$S_{a,1s}$
JGB 292	#983	1.30 *g*	#1703-3	0.14 *g*
NWH 360	#1044	1.17 *g*	#1670-4	0.17 *g*
RRS 318	#1063	1.83 *g*	#1728-2	0.16 *g*
SCE 281	#1085	0.81 *g*	#1737-5	0.11 *g*

Christchurch 2010/2011 foreshock-mainshock

	9 Sept 10		**21 Feb 11**	
Station/Dir	RSN	$S_{a,1s}$	RSN	$S_{a,1s}$
CBGS S01W	#6887	0.35 *g*	#8063	0.69 *g*
CCCC N64E	#6888	0.32 *g*	#8064	0.77 *g*
CHHC N01W	#6889	0.39 *g*	#8066	0.76 *g*
CMHS N10E	#6890	0.51 *g*	#8067	0.93 *g*

Kumamoto 2016 foreshock-mainshock-aftershock

	14 Apr	**15 Apr**	**16 Apr**	**16 Apr**
Station/Dir	$S_{a,1s}$	$S_{a,1s}$	$S_{a,1s}$	$S_{a,1s}$
KMM006 EW	0.46 *g*	0.24 *g*	1.08 *g*	0.18 *g*
KMM008 EW	0.40 *g*	0.38 *g*	1.19 *g*	0.21 *g*
KMMH14 EW2	0.48 *g*	0.48 *g*	0.87 *g*	0.17 *g*

= Mainshock

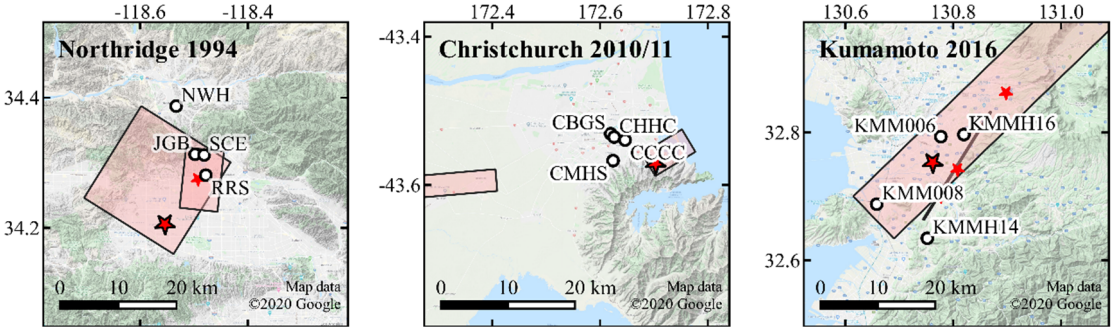

Fig. 5 – Multievent sequences

3. Numerical results

3.1 Trilinear idealization study

Incremental dynamic analysis (IDA) was conducted using the FEMA 695-FF suite, with the intensity measure taken as the 5% damped spectral acceleration at the 3 or 6 story model's fundamental period, and the demand measure taken as the peak interstory drift, residual drift or peak floor acceleration. For this section, the **TRI** model and trilinear material are adopted, with the yield drifts $\delta_{y,L}$ and $\delta_{y,H}$, and yield forces $N_{y,L}$ and N_y normalized to first yield force ($N_{y,L}$ / N_y) and HYP yield displacement ($\delta_{y,H}$ / δ_y) ratios used for comparison and δ_y representing the yield displacement of a bilinear conventional BRB.

The IDA curves are shown in Fig. 6. Major reductionss in residual drift are obtained up to the design level spectral acceleration (1.4 *g* for the 3 story models, 1.0 *g* for the 6 story models) when $N_{y,L}$ / N_y < 1.0 and $\delta_{y,H}$ / δ_y > 1.0, which represent MS-BRBs. There are two cases of particular interest, the "max multistage design" ($N_{y,L}$ / N_y = 0.3 and $\delta_{y,H}$ / δ_y = 3.0) and the "optimal multistage design" ($N_{y,L}$ / N_y = 0.7 and $\delta_{y,H}$ / δ_y = 2.5). The optimal multistage designs withstand 0.21~0.23 *g* greater spectral acceleration before exceeding 0.5% residual drifts. Despite having a slightly higher first yield force $N_{y,L}$ and slightly lower second stage yield drift $\delta_{y,H}$, the residual drift performance is better than the max multistage designs. Similarly, the peak interstory drifts do not increase for the optimal multistage designs, but do increase for the max multistage designs in rare earthquakes. Finally, peak floor accelerations decrease as $N_{y,L}$ / N_y decreases.

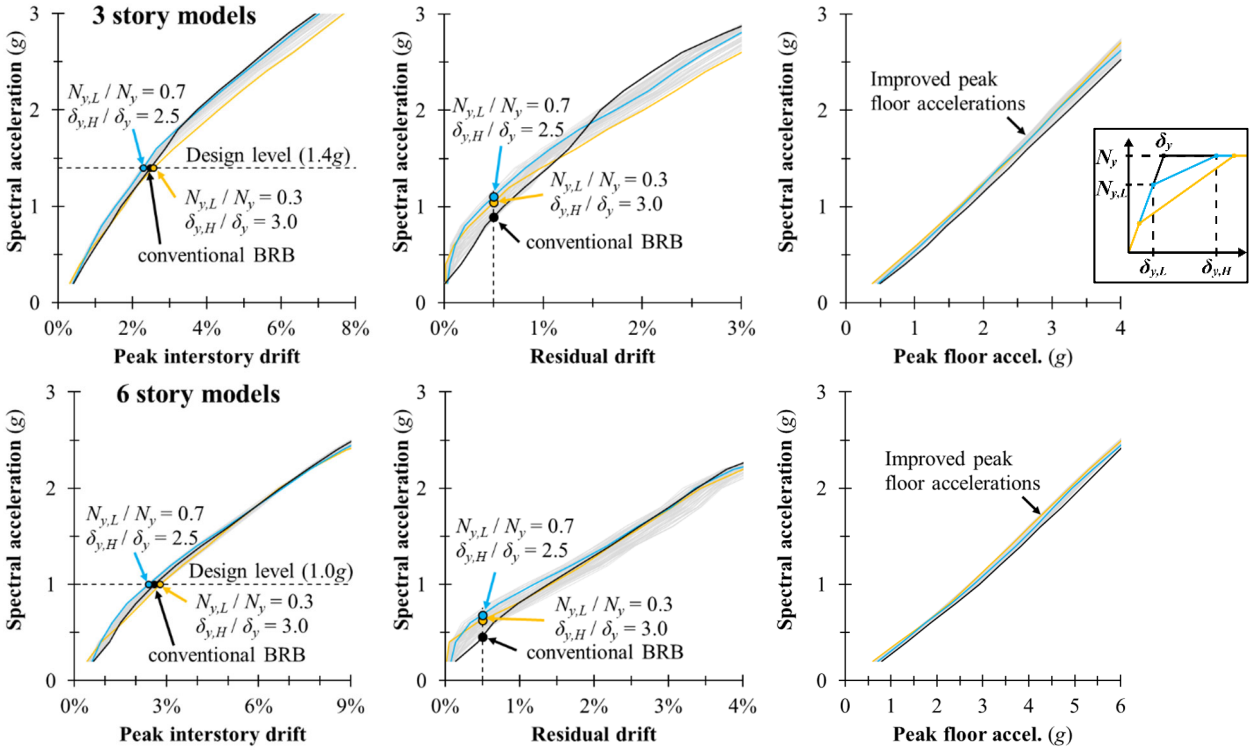

Fig. 6 – Mean IDA curves (FEMA 695-FF suite)

It is also instructive to compare the peak interstory drift to the residual drift from the mean IDA results, as shown in Fig. 7. This indicates that 0.5% residual drifts occur after 15% greater peak interstory drifts for the optimal multistage designs, and at still larger peak interstory drifts for the max multistage designs. However, the max multistage design results are offset by the larger peak interstory drifts at a given ground motion intensity for these models.

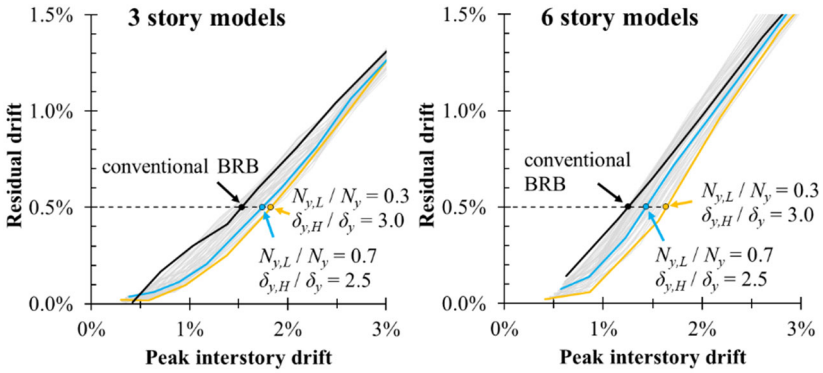

Fig. 7 – Mean IDA drift comparison (FEMA 695-FF suite)

Simply maximizing the separation in yield displacements ($\delta_{y,H} / \delta_{y,L}$) does not necessarily result in the best performance, as suggested by previous researchers [6]. Therefore, the reduction in residual drift is examined for the full parameter matrix of $N_{y,L} / N_y$ and $\delta_{y,H} / \delta_y$ in Fig. 8. This indicates that increasing the HYP yield displacement is effective up to about $\delta_{y,H} / \delta_y = 2.5$, at which point there are diminishing returns. However, reducing the first yield force produces a local optima around $N_{y,L} / N_y = 0.7$, with a small reduction in $N_{y,L}$ clearly desirable and required to achieve a trilinear hysteresis, but the energy dissipation of the LYP cores becoming ineffective when $N_{y,L}$ is too small. While these trends are pronounced for intensities below the design level, an extremely small $N_{y,L} / N_y$ ratio even becomes detrimental to performance relative to a conventional BRB under severe ground motions. Note that $N_{y,L}$ primarily depends on the LYP core material's yield strain and yield length, rather than core area.

Therefore, designers should seek to achieve $0.5 < N_{y,L} / N_y < 0.8$ and $\delta_{y,H} / \delta_y > 2.0$ when selecting the core materials, yield lengths and areas for MS-BRBs, but target $N_{y,L} / N_y = 0.7$ and $\delta_{y,H} / \delta_y = 2.5$, if possible.

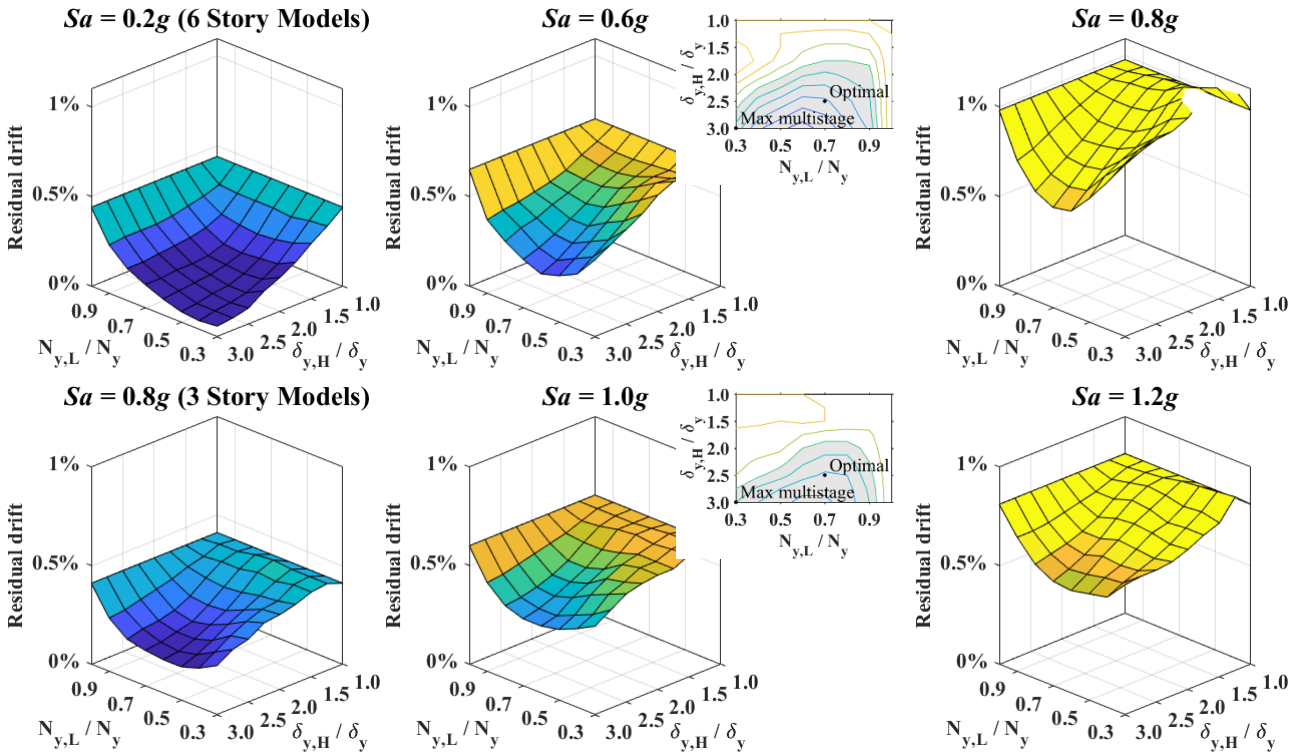

Fig. 8 – Residual drift reduction

3.2 Nonlinear material model

There are several combinations of core materials and yield lengths that could achieve an optimal MS-BRB design of $\delta_{y,H} / \delta_y = 2.5$ and $N_{y,L} / N_y = 0.7$. However, the candidate materials (LY100 and LY225) for the LYP cores exhibit significantly different isotropic hardening properties, which may or may not be effective in reducing residual drift. Therefore, 6 story models of conventional and multistage BRBFs were designed to investigate this effect, using multievent earthquake sequences to amplify the isotropic hardening.

Of particular note is the MS-BRBF-L model, which employs LY100. This was designed with a suboptimal $N_{y,L} / N_y = 0.34$, but the first yield force then increases to $N_{y,L} / N_y = 0.56$ after $+100\% \cdot f_y$ isotropic hardening and to $N_{y,L} / N_y = 0.72$ after $+200\% \cdot f_y$ isotropic hardening, which corresponds to +25% and +50% increases in the gross yield strength. Although this suggests that the MS-BRBF-L model should perform better than the LY225 MS-BRBF model, the increased gross yield strength diminishes the normalized HYP yield drift to less than $\delta_{y,H} / \delta_y < 1.6$, which Fig. 8 suggests is insufficient to realize the benefits of the multistage effect.

The multistage effect is illustrated by Fig. 9, which compares the ground story hysteresis of the 3-story BRBF and MS-BRBF models to the Northridge Newhall mainshock. The low post-yield stiffness of the conventional BRB results in an asymmetric hysteresis that accumulates large residual deformations. Conversely, the MS-BRB HYP core remains elastic in all but one cycle and provides a restoring force that helps maintain a relatively centered hysteresis, while the LYP core dissipates the earthquake's energy. This is a dynamic effect that relies on the separation between the yielding stages.

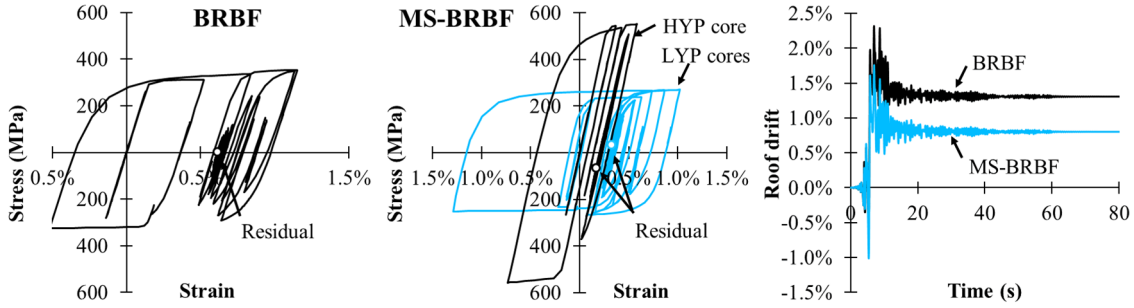

Fig. 9 – Core stress-strain hysteresis (Northridge NHW, ground story BRBs)

Pushover curves (excluding isotropic hardening) and mean interstory drift distributions under the FEMA 695-FF suite (scaled to $S_a = 0.8g$) are depicted in Fig. 10. Note that the initial stiffness and gross yield strength are identical for the BRBF, MS-BRBF-L, MS-BRBF, and MS-BRBF-H models, while the BRBF-L model has a 25% lower strength. The MS-BRBF models experience similar peak interstory drifts as the BRBF models, but smaller residual drifts, which are lowest for the MS-BRBF-L and MS-BRBF-H models.

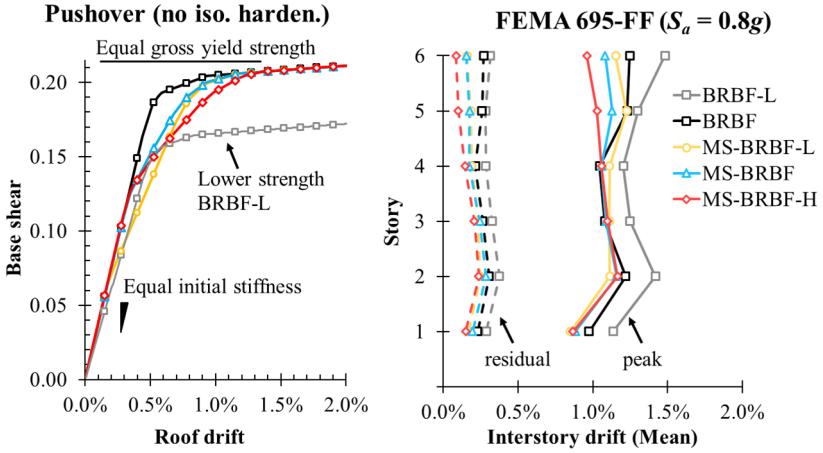

Fig. 10 – Pushover and typical design level responses (6 story models)

3.3 Multievent earthquake sequence

Three sets of multievent earthquake sequences were analysed to investigate the effect of isotropic hardening on the residual drift. Representative roof drift timeseries for the unscaled sequences are shown in Fig. 11, with the Northridge and Christchurch sequences consisting of a strong mainshock and a weaker aftershock or foreshock. However, the Kumamoto sequence is unique in that it includes multiple strong events.

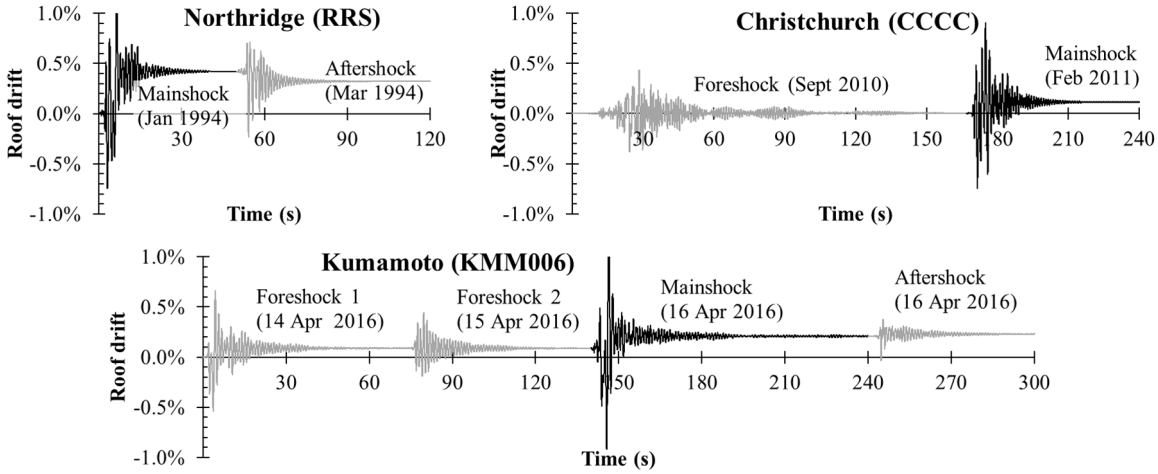

Fig. 11 – Earthquake sequences

The peak interstory drift and residual drift at the end of each stage is shown in Fig. 12 for the three different earthquake sequences. All MS-BRB models exhibited significantly lower residual drifts than the conventional BRBF models, with the MS-BRBF-H model (LY225 + SA630B) performing the best. However, yielding during foreshocks diminished the residual drift reduction effect of the MS-BRBF-L models, which actual performed worse than the MS-BRBF model during the Kumamoto sequence, despite exhibiting significantly greater overstrength.

The poor performance of the MS-BRBF-L model may be explained by the severe isotropic hardening of the LY100 cores, which gradually shifts the multistage parameters outside of the optimal range, effectively producing a stronger, but conventional BRBF. This suggests that the multistage effect is at least as effective in reducing residual drifts as strain hardening. However, isotropic strain hardening in the MS-BRBF-L model produced large overstrength forces, negating a key benefit of BRBs.

Therefore, LY100 is not recommended for MS-BRBs, with LY225 preferred for the LYP core.

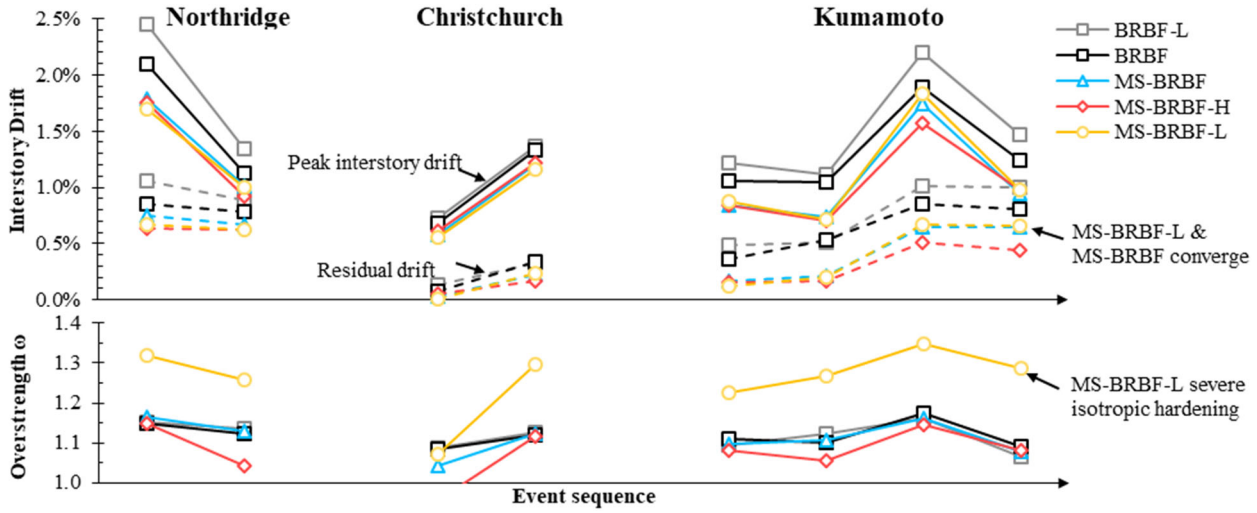

Fig. 12 – Effect of isotropic hardening over multiple events (6 story models)

4. Discussion

4.1 Target yield drifts and strength ratios

The parametric study of idealized trilinear models indicates that increasing the HYP core yield drift has the greatest effect in reducing residual drifts, but with diminishing returns for $\delta_{y,H} / \delta_y > 2.5$. This is primarily achieved by increasing the HYP core steel grade, and corresponds to a HYP yield drift on the order of 0.5%.

Conversely, the optimal first yield force ratio is achieved at $N_{y,L} / N_y = 0.7$, although good performance is also obtained for $0.5 < N_{y,L} / N_y < 0.8$. Both residual and peak interstory drifts are penalized for $N_{y,L} / N_y < 0.3$, which may also result in yielding in ultimate wind events. Therefore, designers should not seek to excessively reduce the LYP yield displacement, which controls $N_{y,L} / N_y$, and instead target a value close to $N_{y,L} / N_y = 0.7$. This may be achieved using a low yield point steel material and / or shorter LYP core yield length.

4.2 Core material selection

While it is necessary to reduce the first yield force, materials with severe isotropic hardening (e.g., LY100) should be avoided. This not only incurs a penalty in greater overstrength forces, but also diminishes the multistage effect in subsequent events, such as when yielding occurs during a strong foreshock or a second large earthquake later in the building's life. It was also found that isotropic hardening is less effective in reducing residual drifts that the multistage effect. Therefore, LY225 with a reduced core yield length is recommended for the LYP core.

The HYP core should achieve yield displacements on the order of 2.0 ~ 2.5 times that of a conventional SN400B BRB, which is just barely feasible with SA440B. The optimal yield displacement of $\delta_{y,H} / \delta_y = 2.5$ would require either increasing the HYP core yield length or using SA630B. Although the prescriptive provisions of most seismic design codes [15] prohibit using these high strength steel grades in plastic regions, relatively low strain demands are expected in the HYP core and BRBs are qualified through physical testing, which is typically permitted as an exception to these provisions.

4.3 Proposed design procedure

Assuming that the LYP yield force is at least $N_{y,L} / N_y > 0.5$, the IDA curves indicate that the peak interstory drifts are lower in MS-BRBs compared to conventional BRBs with equal initial stiffness and gross yield strength. This holds at up to several multiples of the design intensity, suggesting that current R and Cd factors used for conventional BRBs may be directly applied to this class of MS-BRBs, with the improved residual drift performance taken as an implicit benefit. Therefore, a simple design procedure is proposed:

Step 1) Calculate the required force with the same ductility factor (e.g., R = 8) as used for conventional BRBs. Check this against the MS-BRB gross yield strength (sum of core areas × yield strengths).

Step 2) Select the LYP and HYP core materials and yield lengths to achieve $0.5 < N_{y,L} / N_y < 0.8$ and $\delta_{y,H} / \delta_y > 2.0$, but target $N_{y,L} / N_y = 0.7$ and $\delta_{y,H} / \delta_y = 2.5$, if possible. Do not use materials with severe strain hardening, such as LY100.

Step 3) Check that the first yield force $N_{y,L}$ exceeds the ultimate wind force demand. Note that $N_{y,L}$ includes a contribution from the HYP core.

Equations to derive $N_{y,L}$, N_y, $\delta_{y,L}$ and $\delta_{y,H}$ in Steps 2 and 3 are outside the scope of this paper, but are presented in other work by the authors.

5. Conclusions

A novel multistage buckling-restrained brace is introduced to reduce residual drifts in simply supported BRBFs, and the optimal design parameters investigated using archetype frame models.

- Multistage BRBs reduce residual drifts when the LYP and HYP core materials, areas and yield lengths are proportioned to achieve a first yield force ratio of $0.5 < N_{y,L} / N_y < 0.8$ and a HYP yield drift ratio of at least $\delta_{y,H} / \delta_y > 2.0$, while optimal performance is achieved when $N_{y,L} / N_y = 0.7$ and $\delta_{y,H} / \delta_y = 2.5$.
- Materials with severe isotropic hardening diminish the multistage effect and increase overstrength, which is less effective in reducing residual drifts than a stable multistage effect. Therefore, LY100 is not recommended for the LYP core.

References

[1] Iwata Y, Sugimoto H, Kuwamura H (2006): Reparability limit of steel structural buildings based on the actual data of the Hyogoken-Nanbu Earthquake. *38th Joint Meeting of the U.S.-Japan Panel on Wind and Seismic Effects, NIST SP1057*, Gaithersburg, Maryland, United States.

[2] McCormick J, Aburano H, Ikenaga M, Nakashima M (2008): Permissible residual deformation levels for building structures considering both safety and human elements. *14th World Conference on Earthquake Engineering*, Beijing, China.

[3] Sitler B, Takeuchi T, Ryota M, Terashima M, Terazawa Y: Experimental investigation of a multistage buckling-restrained brace. Manuscript submitted for publication.

[4] Wada A, Connor J, Kawai H, Iwata M, Watanabe A (1992): Damage tolerant structure. *5th U.S.-Japan Workshop on the Improvement of Building Structural Design and Construction Practices, ATC-15-4*, San Diego, United States.

[5] Saeki E (1997): *Hysteresis characteristics of steels and buckling restrained unbonded braces*. PhD Dissertation, Tokyo Institute of Technology. (in Japanese)

[6] Atlayan O, Charney F (2014): Hybrid buckling-restrained braced frames. *Journal of Constructional Steel Research,* **96**, 95–105.

[7] Sun J, Pan P, Wang H (2018): Development and experimental validation of an assembled steel double-stage yield buckling restrained brace. *Journal of Constructional Steel Research,* **145**, 330-340.

[8] Li GQ, Sun YZ, Jiang J, Sun FF, Ji C (2019): Experimental study on two-level yielding buckling-restrained braces. *Journal of Constructional Steel Research*, **159**, 260–269.

[9] Miller D, Fahnestock L, Eatherton M (2012): Development and experimental validation of a nickel-titanium shape memory alloy self-centering buckling-restrained brace. *Engingeering Structuctures*, **40**, 288–298.

[10] Sabelli R, Mahin S, Chang C (2003): Seismic demands on steel braced frame buildings with buckling-restrained braces. *Engineering Solid Mechanics*, **25**, 655–666.

[11] McKenna F, Fenves G, Scott M (2000): *Open System for Earthquake Engineering Simulation (OpenSees)*. Pacific Earthquake Engineering Research Center, University of California, Berkeley.

[12] American Society of Civil Engineers (2016): *Minimum design loads and associated criteria for buildings and other structures, ASCE/SEI 7-16*.

[13] Yamazaki H, Kasai K, Ono Y, Kaneko H, Sadasue K (2006): Curved hysteresis model of structural steel under cyclic loading, *AIJ Annual Convention*, . (in Japanese)

[14] Federal Emergency Management Agency (2009): *Quantification of building seismic performance factors, FEMA695*.

[15] American Institute of Steel Construction (2016): *Seismic provisions for structural steel buildings, AISC 341-16*.

